Final report on OTKA NN project 130004 “Development of High CO-Tolerant Anode Electrocatalysts for Reformate-Fed PEM Fuel Cells (ELECTROCAT)”

1. Main tasks of the project

Our goals in this research project were threefold. First, the material science knowledge of multicomponent oxides and previous experience of our research group in the development of W-containing composite materials was used to create novel $Ti_{(1-x)}M_xO_2$-C (M: Mo, Nb, Sn; x: 0-0.4) mixed oxide and various carbonaceous materials composite supports for use as CO-tolerant anode electrocatalysts with different Pt content in polymer electrolyte membrane fuel cells (PEMFCs). Our aims required the development of well controlled and highly reproducible sample preparation methods. Secondly, the Turkish partner developed a technology for integrating these novel oxide-containing platinum electrocatalysts into Membrane Electrode Assemblies (MEAs). The aims also included studies of the performance of MEAs assembled into a single fuel cell and 5-cell PEMFC stacks, both under realistic operating conditions and under simulated CO poisoning conditions.

2. Main results of the project

The research work in the project was performed in three work packages. Work Package 1 focused on the development of novel CO-tolerant electrocatalysts. In this work package novel composites consisting of titania-based mixed oxides and different surface modified carbonaceous materials were prepared to find the best support for the electrocatalysts. In Work Package 2 the technology of integrating the novel electrocatalysts into membrane-electrode assemblies (MEAs) by spray and painting methods were developed and the most promising systems were selected for fuel cell tests. In Work Package 3 MEAs and other components (bi-polar plates, current collection plates and gaskets) were assembled into fuel cells and tested under realistic working conditions and simulated CO poisoning conditions. Work Package 1 contained the tasks of the Hungarian partner, activity in Work Package 2 was shared between the Hungarian and the Turkish partner and Work Package 3 was performed by the Turkish partner.

2.1 Design of novel mixed oxide–carbon composite supports for Pt-based electrocatalysts

2.1.1 Design of Ti–Mo mixed oxide–carbon composite supports for Pt-based electrocatalysts

One of the main tasks of the project was to assess the effect of different carbonaceous backbone materials on the properties and performance of the Mo-doped TiO_2-carbon composite supported electrocatalysts. During the research work it turned out that slight modification of the synthesis procedure is needed depending on the properties of the different carbon materials. The results of this work were summarized in six publications [1-6].

In addition, certain peculiarities of the Mo-Pt interaction, determining the CO tolerant behaviour of the electrocatalysts, were also explored (publication [7]).

2.1.1.1 Effect of the functionalization and the type of carbonaceous materials in composite supported Pt catalysts on the electrocatalytic performance

It is well known that inert surface of carbon requires suitable chemical modification to increase its hydrophilicity and, additionally, to improve the interaction between the support surface and the metal oxide. In our recent study [1] the functionalization of commercial carbon (**BP**: Black Pearls 2000 (Cabot)) was done by either a one-step treatment with glucose or by a two-step treatment with HNO_3 and glucose. In some cases before functionalization carbon was pre-treated in nitrogen at 1000 °C for 3 h. According to the thermogravimetric (TG) and XPS measurements it can be stated that the amount and type of the surface oxygen groups formed (strong and/or weak acid groups) mainly depends on the type of the oxidizing/functionalizing reagent used. Pre-treatment in nitrogen at 1000 °C for 3 h before functionalization results in further increase of the amount of oxygen-containing groups.

Taking into account the peculiarities of various carbonaceous materials, the synthesis procedure of the mixed oxide–carbon composite type electrocatalyst supports with 75/25, 50/50 and 25/75 oxide/carbon mass ratio was successfully optimized for use of Vulcan XC-72 (**V**), commercial (**BP**) and functionalized (**F-BP**) carbon materials [1-3]. The multistep sol-gel-based synthesis method was

also adapted to obtain exfoliated graphite oxide (**GO**)-derived composite with 25 wt.% GO and rutile-TiO_2 structure.

Table 1 contains abbreviation and nominal composition details of the $Ti_{0.8}Mo_{0.2}O_2$-C composite supported 20 wt.% Pt electrocatalysts studied in ref. [2]. It was demonstrated that the time and temperature of aging and maintenance of the appropriate acidic pH during the synthesis played key role in exclusive formation of the rutile phase, which is essential for good Mo incorporation and enhanced stability. As demonstrated by XRD, almost complete incorporation of the Mo-dopant into substitutional sites of the TiO_2 lattice, which protect the doping metals from dissolution, was achieved.

Table 1. The influence of the composition and microstructure of the Pt/$Ti_{0.8}Mo_{0.2}O_2$-C catalysts on the electrocatalytic performance

Sample [a]	**Nominal composition**	S_{BET}, m^2/g [b]	$E_{CO,max}$, [c] mV	$ECSA_1$, m^2/g_{Pt}	$\Delta ECSA_{500}$, % [d,e]	$\Delta ECSA_{10,000}$, % [d]
Pt/25BP	75$Ti_{0.8}Mo_{0.2}O_2$-25C	248	705 (*sh:* 745)	81.6	7.4	37.0
Pt/50BP	50$Ti_{0.8}Mo_{0.2}O_2$-50C	411	705 (*sh:* 745)	79.2	8.6	34.1
Pt/75BP	25$Ti_{0.8}Mo_{0.2}O_2$-75C	1120	775	69.1	11.8	27.6
Pt/25F-BP	75$Ti_{0.8}Mo_{0.2}O_2$-25C	147	705 (*sh:* 745)	60.9	7.0	30.5
Pt/50F-BP	50$Ti_{0.8}Mo_{0.2}O_2$-50C	455	705 (*sh:* 745)	67.6	7.3	31.2
Pt/75F-BP	25$Ti_{0.8}Mo_{0.2}O_2$-75C	726	775	65.4	11.2	24.1
Pt/25V	75$Ti_{0.8}Mo_{0.2}O_2$-25C	47	705 (*sh:* 745)	81.3	9.0	43.6
Pt/50V	50$Ti_{0.8}Mo_{0.2}O_2$-50C	108	705 (*sh:* 745)	73.0	10.1	35.0
Pt/75V	25$Ti_{0.8}Mo_{0.2}O_2$-75C	175	755	83.0	12.2	36.4
Pt/25GO	75$Ti_{0.8}Mo_{0.2}O_2$-25C	130	705 (*sh:* 745)	77.6	8.4	36.0
Pt/C	-	-	795	94.5	12.7	47.8

[a] **BP**: Black Pearls 2000, **V**: Vulcan XC-72; **GO**: Graphite Oxide derived carbon; **F-BP**: BP carbon pre-treated at 1000°C in N_2 for 3 h before functionalization, then functionalized with HNO_3 and glucose [1];
[b] Specific surface area of the composite support materials determined by nitrogen adsorption measurements;
[c] The position of the main CO stripping peak measured on fresh catalysts;
[d] $\Delta ECSA_{500}$ and $\Delta ECSA_{10,000}$ were calculated from the charges originated from the hydrogen desorption in the 1st and 500th or 10,000th cycles: $\Delta ECSA_N = \{1-(ECSA_N/ECSA_1)\}\times 100\%$;
[e] $\Delta ECSA_{500}$ values were calculated from the 10,000-cycle stability measurements;
sh= shoulder.

As shown in Table 1 with increasing carbonaceous material content in the composites, an increase in the specific surface area (SSA) was observed. In the samples with high carbon content the carbonaceous backbone behaves as a good hard template leading to homogeneous distribution of mixed oxide particles/layers over carbon, which has been confirmed by TEM measurements. The appearance of well dispersed, uniformly distributed Pt on the surface of the all catalysts studied was evidenced by TEM; the type of used carbonaceous materials practically did not affect the average Pt particle size.

Functionalization of carbon modified in some extent the nucleation and growth of the rutile-TiO_2 phase on carbon materials, which may have some beneficial effect on mixed oxide coating of the carbonaceous backbone. In addition, the decrease of the S_{BET} of the composites prepared using F-BP materials (see Table 1), independently on the content of carbonaceous material, can be an indication on the formation of more homogeneous mixed-oxide coating comparing to the samples prepared using unmodified BP.

The values of the electrochemically active Pt surface area ($ECSA_1$) presented in Table 1 were calculated from the charge transfer accompanying the hydrogen desorption taking into account the capacitive currents, originated from double layer charging of the CVs in the first cycle. As shown in Figs. 1.A and 1.C, the functionalization of carbon results in some decrease of the ECSA of corresponding Pt catalysts. Figs. 1.B and 1.D show that the oxidation of CO on these Pt/$Ti_{0.8}Mo_{0.2}O_2$-C catalysts commences at exceptionally low potential values (ca. 50 mV). The electrochemical stability tests for 500 polarization cycles performed on the catalysts studied in this work revealed that the smallest performance loss ($\Delta ECSA_{500}$) was observed on the Pt/25F-BP catalyst with $Ti_{0.8}Mo_{0.2}O_2$/C mass ratios of 25/75 (see Table 1).

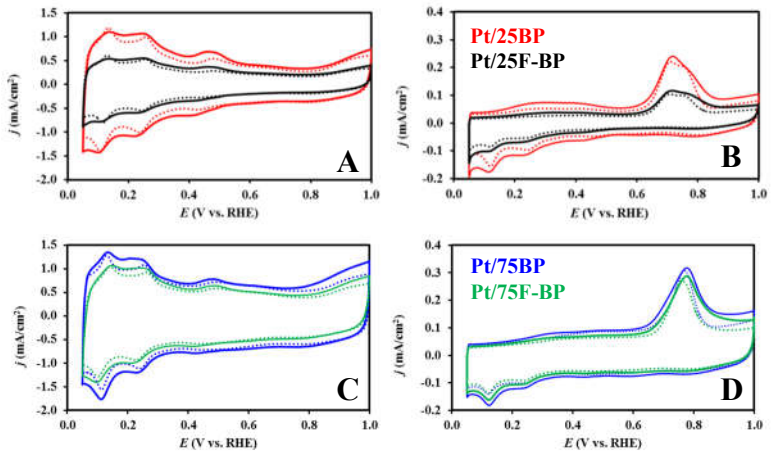

Fig. 1. Effect of the functionalization procedure of carbon on the electrocatalytic performance. Cyclic voltammograms (A, C) and Ar-purged CO_{ads} stripping voltammograms (B, D) of the electrocatalysts recorded before (solid line) and after 500 cycles (dashed line) of the stability test. Nominal composition of the electrocatalysts was presented in Table 1. Obtained in 0.5 M H_2SO_4 at 100 mV/s (A, C) and 10 mV/s (B, D), T = 25 °C.

Electrochemical investigations revealed significantly improved CO-tolerance and stability for the composite supported electrocatalysts compared to the Pt/C reference system (see Table 1). However, characteristic performance differences were found between the catalysts with different mixed oxide/carbon ratio. As the key requirement for CO tolerance is an intimate interaction between the surface Mo species and the Pt nanoparticles, composites containing 50 or 75 wt.% mixed oxide exhibited better initial CO-tolerant behavior. However, as shown in Fig. 2, long-term stability tests suggested improved behavior for the catalysts with higher carbon content, indicating that the more homogeneous microstructure observed for these catalysts may be the key for enhanced stability. At the same time, the type of the carbonaceous material seemed to play a smaller role in determining the stability of the catalysts, although Black Pearls-based supports performed typically better [2,3].

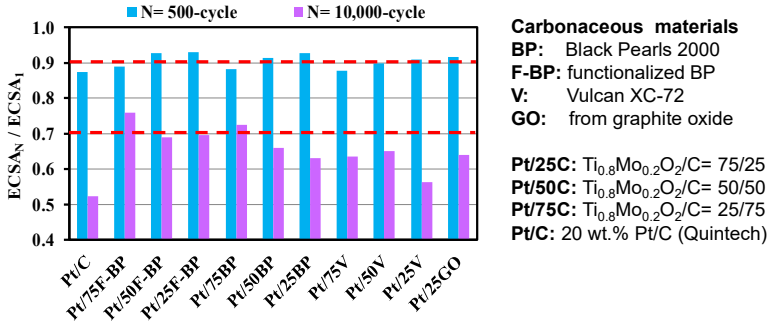

Fig. 2. Comparison of the electrochemically active Pt surface area loss (ΔECSA) of the reference 20 wt.% Pt/C and composite supported Pt catalysts as a function of the number of cycles: 500-cycle ( ) and 10,000-cycle ( ).

Taking into account that upon application in fuel cells the high oxide content in the catalyst layer can lead to a slight increase of the cell resistance, our results indicate that the Pt/75BP and Pt/75F-BP electrocatalysts with $Ti_{0.8}Mo_{0.2}O_2$/C= 25/75 ratio are more promising for general use.

These results were used in the BSc theses "Preparation of novel composite support materials for CO tolerant and stable anode electrocatalysts" of Khirdakhanim Salmanzade presented at the Budapest University of Technology and Economics in 2020.

2.1.1.2 Peculiarities of the preparation of composites containing carbon materials of a new type as supports of electrocatalysts

Graphite oxide derived TiO_2-carbon composite supports

Graphite oxide can be regarded as an ultimate case of functionalized carbon materials. Because of its extremely high functional group content, its delamination and handling in sol-gel synthesis is

much easier than that of other, more hydrophobic carbons. The aim of this study was to provide insight into carbonaceous phase related issues by comparing the structural and functional properties of TiO_2-C composites with TiO_2/C= 75/25 mass ratio prepared by multistep sol-gel method on GO-derived and BP carbon black materials [4]. Our further aim was to achieve the exclusive formation of the rutile-TiO_2 phase in these composites, as the ultimate goal in our future work is to use these knowledge to prepare various transitional metal M (M: Mo, Sn, Nb)-doped TiO_2-GO derived carbon composites as potential catalyst supports for Pt electrocatalysts in PEMFCs.

GO was prepared from graphite by the Hummers-Offeman method. In order to adapt the composite preparation method for GO we had to overcome the following difficulties: (1) strong acidic media is necessary for the formation of the rutile nuclei (consequently to Mo incorporation), in contrast the mild basic media is necessary for the delamination of GO. We proved by XRD measurements that addition of 5 hours aged solution of titanium isopropoxide in to delaminated GO with vigorous stirring resulted in exclusively rutile phase of mixed oxide after high-temperature treatment (HTT). The BET specific surface area was 264 m^2/g, which corresponds to the requirements for electrocatalyst carriers. (2) Upon usage of our conventional preparation method, $NaNO_3$ crystallized in the presence of delaminated GO, which decomposed with oxygen formation under HTT needed to incorporate Mo in to the rutile phase leading to uncontrolled treatment conditions. Therefore, the liquid phase was changed in the slurry and the solid part was washed before the Mo precursor was added. XRD measurements proved that $NaNO_3$ was removed. (3) GO plates may be fractured during HTT. Therefore, a solvothermal treatment in *i*-PrOH was added as new step before HTT, which has been reported to enhance formation of a more stable reduced graphene oxide (r-GO) structure. ^{13}C NMR analysis proved that the carbon structure of these composites is more graphitic without functional groups.

Based on the results of XPS and TEM, it can be concluded that, regardless of the carbon source, sintering of titania during HTT of TiO_2-C composites leads to the formation of relatively large crystallites with incomplete coverage of the carbon backbone. In good agreement with these results, electrochemical studies have shown that the presence of the 75 weight% TiO_2 in the BP and GO-derived TiO_2-C composite does not significantly affect the performance of related Pt catalysts. Long-term stability tests carried out in the potential range 50 <E < 1000 mV showed that the stability of catalysts under these conditions mainly depends on the properties of the active phase (i.e., Pt NPs), while the effect of the composite support is limited. The Pt/TiO_2-GO derived sample showed higher ORR activity than the Pt/TiO_2-BP derived one. Based on the decrease of electrochemical surface area, the stability order was the following: Pt/C (commercial) < Pt/TiO_2-BP derived C < Pt/TiO_2-GO derived C.

Multi-layer graphene containing composite supports

Another promising novel carbon material is multilayer graphene (MG), which can be relatively easily prepared from graphite. Ball milling is a relative simple and promising technique for preparation of inorganic oxide – carbon type of composites with MG-like carbonaceous part. In ref. [5] novel TiO_2-MG and $Ti_{0.8}Mo_2O_2$-MG type of composites were prepared by ball milling of graphite in order to get electrocatalyst supports for PEMFCs. Starting rutile TiO_2 was obtained from P25 by heat treatment in air at 1000 °C for 2 hours. As starting material for Mo-containing MG-type supports a series of $Ti_{0.8}Mo_2O_2$–BP composites was prepared using our previously developed multistep sol-gel method, with nominal BP carbon content of 0, 5, 10, 25 wt.%, in composites PC0, PC05, PC10, PC25, respectively. This was necessary as carbon-free sol-gel-prepared $Ti_{0.8}Mo_{0.2}O_2$ does not have the necessary specific surface area.

As a second step, graphite was ball-milled with the parent composites (PC05, PC10, PC25) or TiO_2 in the presence of glucose in a planetary ball milling machine at room temperature. Ball milling of TiO_2 or parent composites with graphite resulted in catalyst supports with enhanced carbon content and with appropriate specific surface area. XRD and Raman spectroscopic measurements indicated the changes of graphite during the ball milling procedure while the oxide part remained intact. TiO_2-MG obtained from graphite by ball milling contained carbonaceous part of crystallite size ~10 nm calculated from the Raman spectrum (see Fig. 3.A). TEM images proved that platinum existed in the form of highly dispersed nanoparticles on the surface of both the Mo-free and of Mo-containing electrocatalyst. Elemental maps indicated that Pt nanoparticles preferred the oxide part of the

composite-type support. The Mo element map was slightly more diffuse than the Ti element map which was attributed to the strong mechanical effects during the grinding of the mixed oxide.

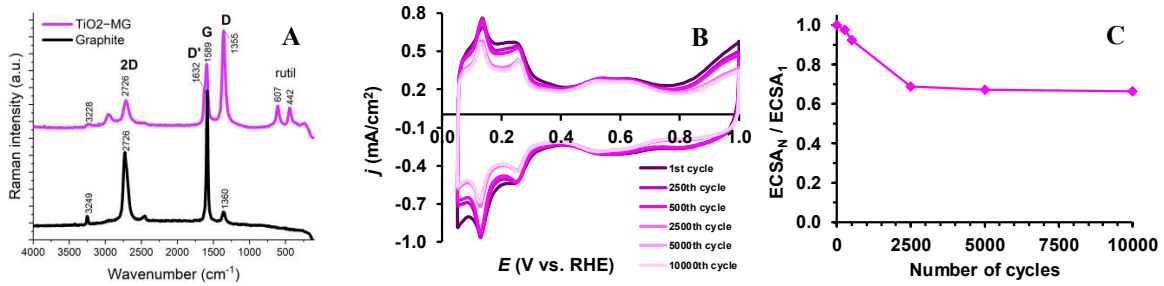

Fig. 3. Characterization of TiO_2-MG sample with the TiO_2/MG= 25/75 mass ratio: (A) Raman spectra of the composite support, (B) cyclic voltammograms of 20 wt.% Pt/TiO_2-MG electrocatalyst obtained during long-term stability test involving 10,000 polarization cycles and (C) comparison of the electrochemically active Pt surface area measured after N cycles normalized to ECSA measured in the 1st cycle ($ECSA_N/ECSA_1$) as a function of the number of cycles (N).

Electrocatalytic performance of the catalysts loaded with 20 wt.% Pt was studied by cyclic voltammetry, CO_{ads}-stripping voltammetry done before and after the 500-cycle stability test, as well as by the long-term stability test involving 10,000 polarization cycles. Cyclic voltammograms of the Pt/$Ti_{0.8}Mo_{0.2}O_2$-MG electrocatalysts showed a characteristic redox peak pair between 380 mV and 530 mV, which was assigned to oxidation/reduction of reducible MoO_x surface species indicating an active interface between the Pt NPs and Mo-containing support. The Pt/TiO_2-MG electrocatalyst was more stable in the long term electrocatalytical tests than its Mo-containing analogues. Comparison of the CO_{ads} stripping behaviour of the Pt/$Ti_{0.8}Mo_{0.2}O_2$-MG samples to the Mo-free Pt/TiO_2-MG one demonstrated increased CO tolerance of the Mo-containing catalysts in line with the results of our previous work.

High stability during long-term stability test obtained on the Pt/TiO_2-MG catalyst was demonstrated. Moreover, as shown in Figs. 3.B and 3.C, after 2500 polarization cycles the decrease in the ECSA values on this catalyst was negligible. In addition, it should be noted that long-term stability of Pt/TiO_2-MG catalyst expressed in $ECSA_N/ECSA_1$ (N: number of cycles) (Fig. 3.C) was more favorable compared to that of Pt/C catalyst ($ECSA_{10,000}/ECSA_1$ of ~ 0.5 (see Table 1)).

Comparing the electrochemical behavior of Pt catalysts supported by TiO_2-C composites from different methods, the ball-milled sample containing multilayer graphene has lower ECSA and activity than GO-derived carbonaceous containing catalyst and the commercial Pt/C. However, the stability of both new types of samples is higher than that of commercial Pt/C [6].

Although, we were able to prepare TiO_2-multilayer graphene (TiO_2-MG) composite type of support by ball milling technique [5], however the oxide/carbonaceous material ratio in the support should be optimized regarding the stability and activity of the obtained electrocatalysts. It is known that N-doped graphene can show strong adsorption and keep Pt nanoparticles in highly dispersed form. The aim of work is mapping the applicability of ball milling for support preparation in two case studies: (i) TiO_2-MG composites of different TiO_2 content; (ii) TiO_2-N-doped graphene composites. We attempt to compare the electrochemical behaviour of the catalysts obtained from ball milling- and sol-gel derived supports and commercial Pt/C [6].

It should be emphasized that the accumulated experience has opened up possibilities for using both methods (sol-gel and ball milling) for obtaining composite materials that contain different types of carbonaceous materials, such as graphene nanoplatelets, undoped graphene and N-doped graphene.

These results were used in the MSc theses “Preparation and characterization of Pt based electrocatalysts for PEM fuel cells” of Ilgar Ayyubov presented at the Budapest University of Technology and Economics in 2020.

Moreover, these observations will form the base for the PhD theses “Novel electrocatalysts for PEM fuel cells by use of new type of carbonaceous materials: preparation and characterization” of

Ilgar Ayyubov, who is now a PhD student of the George Oláh Doctoral School of Budapest University of Technology and Economics.

2.1.1.3 Mo-Pt interactions in Mo-doped mixed oxide – carbon composite supported Pt electrocatalysts

The next task of this research project was the use of surface spectroscopic approach to clarify the nature of the active Mo-Pt ensembles in the mixed oxide – carbon composite supported catalysts. According to electrochemical experiments, the electrooxidation of CO at very low potentials in $Ti_{(1-x)}Mo_xO_2$-active carbon composite supported Pt electrocatalysts is explained by the interplay of reducible ionic Mo species and the Pt nanoparticles. By comparing the surface composition/chemical state changes of the electrocatalysts and electrodeposited model Mo/Pt systems upon annealing and reduction, it was established that the sites of the catalysts responsible for CO tolerance are formed in the interfaces of Pt particles and reducible Mo species while the effect of coverage of the Pt particles by Mo is undetectable.

In our recent study [7] the electrochemical studies of the Mo-containing composite supported Pt catalysts were completed by model studies during which Mo was electrochemically deposited onto Pt electrodes. As the first step of the investigations, both the Mo/Pt model sample and the $Pt/Ti_{0.8}Mo_{0.2}O_2$-C catalysts were tested by cyclic voltammetry measurements. The results, in very good agreement with previous findings, confirmed that very similar surface oxidation/reduction processes occur in both systems (Fig. 4).

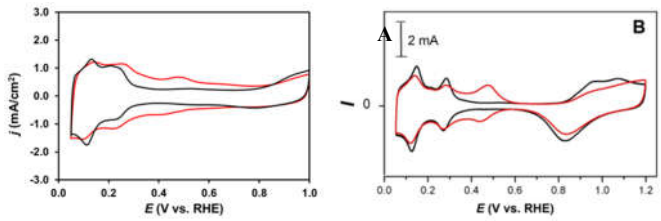

Fig. 4. (A) CV of the 10 wt.% $Pt/Ti_{0.8}Mo_{0.2}O_2$-C catalyst (red curve) and a 10 wt.% Pt/C catalyst (black curve). (B) CV of a Pt electrode recorded in both 0.5 M H_2SO_4 (black curve) and in 5×10^{-4} M Mo^{6+}-containing 0.5 M H_2SO_4 (red curve). For details see ref. [5].

A surface spectroscopic approach was used to clarify the nature of the active Mo-Pt ensembles in the mixed oxide – carbon composite supported catalysts. The results of the annealing/reduction studies performed by photoelectron spectroscopy are summarized in Fig. 5.

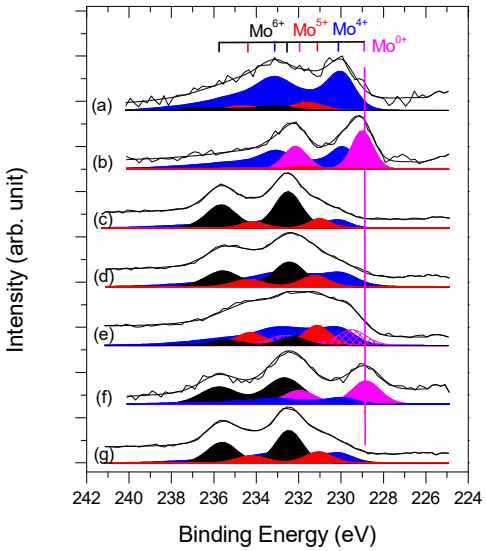

Fig. 5. Mo 3d core level spectra of the Mo/Pt model sample in the initial state (a) and after 100 mbar 1h H_2 exposure at room temperature (b); the 40 wt.% $Pt/Ti_{0.8}Mo_{0.2}O_2$-C catalyst in the initial state (c), after 100 mbar 1 h H_2 exposure at room temperature (d) and at 200 °C (e); the previously reduced Mo/Pt sample after 48 h air exposure at room temperature (f); and the previously reduced catalyst sample after 48 h air exposure at room temperature (g). The assignment of the Mo chemical states is shown on the bar above the graphs.

The upper two traces were obtained on the Mo/Pt model sample in the initial state and after hydrogen exposure at room temperature. The initial state spectrum confirms that the electrochemically deposited Mo is present on the Pt electrode predominantly in the Mo^{4+} ionic state; hydrogen activated on Pt reduces the majority of these Mo ions to the metallic state even upon room temperature exposure. A complete loss of ionic Mo contributions is achieved during hydrogen treatment at 200-300 °C, thus reduction around this temperature is enough for formation of a metallic Mo-Pt surface phase. The binding energy of the Mo $3d_{5/2}$ peak in this alloyed state is at a 0.8-1.0 eV higher value than that in pure metallic Mo [7].

In case of the real catalyst, a mixture of Mo ionic states (Mo^{4+}, Mo^{5+} and a dominant Mo^{6+} contribution) characterizes the initial state. The room temperature hydrogen exposure leads to a significant reduction, resulting in increasing Mo^{5+} and Mo^{4+} contributions on the expense of the Mo^{6+} signals. During annealing in hydrogen at 200 °C a new Mo chemical state arises at lower binding energies than Mo^{4+}, but even this state cannot be identified with metallic Mo bound to Pt.

The lowest traces of Fig. 5 were measured after room temperature air exposure of the previously reduced Mo/Pt model sample and Pt/$Ti_{0.8}Mo_{0.2}O_2$-C catalyst. In case of the model system, the re-oxidation leads to a significantly different situation than the initial state: while a certain part of Mo is transformed to the Mo^{6+} state, a strong metallic contribution is still present, demonstrating that the alloy formation stabilizes Mo to some extent against oxidation. On the other hand, air exposure essentially restores the initial state of the real catalyst.

The presented results indicate that even if Mo^{4+} ions on Pt form a relatively stable system, this system is transformed into a metallic surface alloy upon reduction around 200-300 °C. On the contrary, we were unsuccessful in inducing Mo-Pt alloy formation in case of the real catalyst under the same conditions, which demonstrates that the amount of Mo directly bound to Pt is negligible in this case. Accordingly, while the electrochemical properties of the model system can be explained by interaction between adsorbed Mo ions and adjacent Pt sites, in case of the real catalyst spillover effects between the Pt particles and the support-bound reducible Mo species must be considered.

2.1.2 Design of Ti–Nb mixed oxide–carbon composite supports for Pt-based electrocatalysts

For the preparation of new type of Ti-Nb mixed oxide and activated carbon composites with different compositions the technique we have developed for $Ti_{(1-x)}M_xO_2$-C (M: W, Mo, x: 0.2-0.4) materials was adapted. Upon the preparation of $Ti_{(1-x)}Nb_xO_2$-C (x: 0.1-0.4) composites with $Ti_{(1-x)}Nb_xO_2$/C= 75/25 mass ratio the success of the sol-gel-based multistep synthesis followed by high-temperature treatment (HTT: Ar, 600 °C, 8 h) was controlled by XRD measurements, in which incorporation of Nb is detected as a characteristic distortion of the rutile unit cell. We demonstrated that - regardless of the nominal Ti/Nb ratio used in the synthesis - the degree of niobium incorporation was only 7.8%. Thus, exclusive Nb incorporation into the TiO_2-rutile (R) lattice was achieved only in the composite materials with Ti/Nb= 90/10 atomic ratio, while in the case of the other samples with higher Nb content the incorporation was only partial. In $Ti_{(1-x)}Nb_xO_2$-C ($x \geq 0.3$) composite materials the non-incorporated Nb formed an orthorhombic niobium pentoxide phase (the ratio of Nb-doped rutile to Nb_2O_5 was R/Nb_2O_5= 70/5 and 57/18 for the $Ti_{0.7}Nb_{0.3}O_2$-C and $Ti_{0.6}Nb_{0.4}O_2$-C samples with 75 wt.% of mixed oxide, respectively). In the $Ti_{0.8}Nb_{0.2}O_2$-C sample, Nb_2O_5 was not detected; nevertheless, the presence of amorphous or crystalline NbO_x phase below the detection limit cannot be excluded.

The XPS results suggest that at high temperatures, Nb moves from the surface layer to the bulk phase. It can be assumed that further optimization of temperature and time of the HTT can lead to a much higher incorporation of Nb into the TiO_2-rutile lattice than the currently achieved 7.8%. Based on XRD, XPS and EDX measurements, it was concluded that non-incorporated Nb species accumulate primarily on the surface. According to the nitrogen adsorption measurements the increase of the Nb content in the composites resulted in slight increase of the S_{BET} of the support from 273 to 311 m^2/g.

After loading of $Ti_{(1-x)}Nb_xO_2$-C (x: 0.1-0.4) composite supports with 20 wt.% Pt both XRD and TEM confirmed the appearance of uniformly distributed Pt particles with mean size of about 2.6-3.3 nm. These catalysts were also investigated by SEM and EDX measurements. The Pt content corresponded relatively well to the nominal values. However, with increasing nominal Nb content, increasing Nb loss was detected after Pt loading, which indicates that segregated Nb species are easily

dissolved. Interestingly, the maximal degree of Nb incorporation as measured by XRD (7.8%) corresponds quite well to the bulk Nb content (8.2%) obtained for the $Ti_{0.9}Nb_{0.1}O_2$-C composite by EDX, thus the solubility limit of Nb in rutile-TiO_2 phase seems to be around 8%.

Electrocatalytic performance of the 20 wt.% Pt/$Ti_{(1-x)}Nb_xO_2$-C (x: 0.1-0.4) catalysts was studied by CO_{ads}-stripping and cyclic voltammetry measurements. The shape of the CO_{ads}-stripping voltammograms and the position of the main CO stripping peak was compared to those measured on the CO-tolerant Pt/$Ti_{(1-x)}M_xO_2$-C (M= W, Mo) catalysts. The lack of the so-called pre-peak, which is responsible for low-potential CO oxidation of W- and Mo-containing catalysts, and the shift of the main CO oxidation peak towards more positive potentials (by 90 mV with respect to the main peak of the W- and Mo-doped catalysts) indicate that the Nb-containing catalysts do not have the ability to oxidize CO at low-potentials, so these catalytic systems cannot be recommended for the fuel cell tests under CO poisoning conditions. However, in accordance with the literature data, Pt catalysts on the Nb-containing support have good stability and increased activity in the oxygen reduction reaction (ORR). The best electrocatalytic performance was observed on the 20 wt.% Pt/$Ti_{0.9}Nb_{0.1}O_2$-C catalyst with complete Nb incorporation into the TiO_2 lattice. Influence of the Pt loading (1, 5 and 20 wt.% Pt) on the electrocatalytic performance was studied using $Ti_{0.7}Nb_{0.3}O_2$-C composite.

2.1.3 Design of Ti–Sn mixed oxide–carbon composite supports for Pt-based electrocatalysts

For the preparation of tin-containing composites, the technique previously developed by the research group for Mo-containing composite materials (see Fig. 6) was adapted (route ***A***) [8].

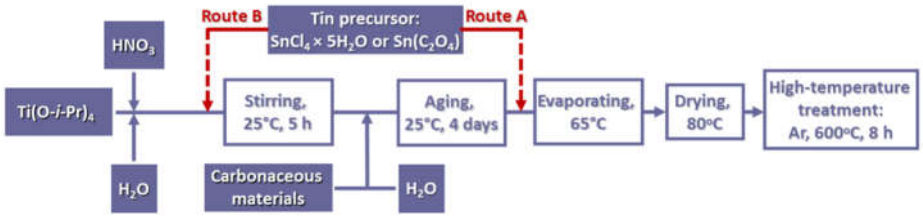

Fig. 6. Preparation steps of $Ti_{(1-x)}Sn_xO_2$-C composites ($Ti_{(1-x)}Sn_xO_2$/C= 75/25 wt.%/wt.%).

XRD, nitrogen adsorption measurements, TEM, SEM/EDX, XPS and Raman spectroscopy were used to characterize the bulk and surface microstructure of the composites and their Pt-loaded counterparts. The change in the TiO_2 lattice parameters measured by XRD, after high-temperature treatment (HTT) at 600 °C, confirmed the incorporation of tin into the rutile unit cell. The degree of Sn incorporation was in good accordance with the amount of tin precursor (for $Ti_{(1-x)}Sn_xO_2$-C with x= 0.1, 0.2 and 0.3, the concentration of tin cations substituting titanium ones, i.e. Sn_{subst}, was 7, 14 and 23%, respectively). TEM investigations indicated the coexistence of large mixed oxide nanorods and their agglomerates with much better dispersed oxide nanoparticles. XPS confirmed that the vast majority of tin was in the +4 oxidation state, although the composite surface shows significant tin enrichment. Presence of metallic Sn in small (1-2%) quantity was revealed in all samples by both XRD and XPS. XPS experiments pointed out that reduction of tin to the metallic state started around 400 °C in Ar atmosphere, which was explained by a carbothermal reduction process. Electrochemical investigations revealed unusually low electrochemically active Pt surface area in the catalysts (~30 m^2/g_{Pt}). Thus, the composites and electrocatalysts obtained in the preparation route ***A*** had the following drawbacks: (i) the formation of a small amount of metallic Sn phase (ii) certain inhomogeneity of the composite materials (the coexistence of $TiSnO_x$ agglomerated in flower-like clusters with more evenly dispersed oxide), and (iii) relatively low electrochemically active Pt surface area [8].

To avoid the formation of Sn^0 and to obtain better oxide homogeneity the synthesis of the composite was modified: the precursor of Sn was introduced immediately after the formation of the transparent Ti-sol, before the addition of the carbon and the aging step (see route ***B*** in Fig. 6).

XRD revealed that these composites contain pure rutile phase; the formation of Sn^0 or SnO_2 was not observed. XPS also suggested the lack of reduced tin species, while indicated better thermal stability of the composite. Based on TEM results, in contrast to the composites prepared by route ***A***, the supports have a more homogeneous/uniform mixed oxide distribution. In particular, the nanorod-

like oxide particles or the flower-like big $TiSnO_x$ agglomerates, characteristic for the composite materials with high mixed oxide content (75 wt.%), were not observed. Instead, faceted oxide particles in the 10-15 nm size range as well as weakly crystallized and/or graphitized C-rich regions were evidenced. The supports were decorated by 2-3 nm metallic Pt particles as confirmed by electron diffraction.

Results of SEM/EDX elemental analysis demonstrated that the Pt content measured by the EDX method in the regions of the catalyst enriched in mixed oxide is in good agreement with the nominal value. This finding indicated that areas rich in Pt and poor in Pt may also exist on the surface of the composite supports and Pt nanoparticles have high affinity to concentrate on the mixed oxide.

The samples obtained by synthesis routes ***A*** and ***B*** were characterized by electrochemical methods including cyclic voltammetry and CO_{ads}-stripping voltammetry measurements combined with stability test involving 500 and 10,000 polarization cycles. Based on the electrochemical results, it can be concluded that the behavior of electrocatalysts strongly depends on the synthesis route used in the preparation of the composite support materials and does not depend on the Ti/Sn ratio. The use of method ***B*** for the preparation of catalysts leads to a noticeable increase in both the ECSA and the activity in CO electrooxidation. The similarity of the shape of voltammograms obtained on the catalysts prepared by both methods allows to assume that similar active species are formed, but in the composites obtained by synthesis route ***B*** the number of these species is higher. An increase of the carbon content in the composite materials prepared by route ***B*** leads to a further increase of the number of catalytically active species responsible for enhanced CO tolerance. Moreover, the similarity of the shape of the CO_{ads} stripping voltammograms to that obtained on alloy-type Sn-Pt/C catalysts gives grounds to assume that the studied composite supported catalysts contain tin in the close vicinity of Pt. Comparison of the electrocatalytic characteristics of Mo- and Sn-containing 20 wt.% $Pt/Ti_{0.8}M_{0.2}O_2$-C electrocatalysts with a high carbon content (75 wt.%) revealed that Sn-containing electrocatalysts can also be promising CO-tolerant anode catalysts for potential use in PEM fuel cells.

These results were used in the MSc theses “Preparation of novel composite support materials for CO tolerant and stable anode electrocatalysts” of Khirdakhanim Salmanzade presented at the Budapest University of Technology and Economics in 2022. Moreover, these results were presented at the 13th International Symposium of the Romanian Catalysis Society (RomCat 2022; Baile Govora, Romania, June 22-24, 2022) [8] and planned to be published after the conference in the Special Issue of the Catalysis Today journal.

2.1.4 Effect of the reductive treatment on the state and electrocatalytic behavior of Pt in catalysts supported on $Ti_{(1-x)}M_xO_2$-C composite (M: Mo, Sn)

It is known that platinum and the oxide form a couple liable for strong metal-support interaction (SMSI) phenomenon, generally manifesting itself in decoration of the metal particles by ultrathin layers of the support material upon annealing under reductive conditions. As the catalytic activity and durability of the TiO_2-supported Pt nanocatalysts are strongly dependent on the SMSI state, the aim of this study is to evaluate this phenomenon as a potential strategy for tailoring the properties of the electrocatalysts supported on $Ti_{(1-x)}M_xO_2$-C (M: Mo, Sn) composite materials.

In our recent study [9] a 20 wt.% $Pt/Ti_{0.8}Mo_{0.2}O_2$-C electrocatalyst with the mass ratio of the mixed oxide to the carbon of 50:50 prepared on Black Pearls 2000 carbon functionalized with HNO_3 and glucose was reduced at 250 °C in H_2 in order to induce SMSI. The electrocatalytic properties and the stability of the original (Pt/50C) and the reduced (Pt/50C-250H) catalysts were analyzed by cyclic voltammetry and CO_{ads}-stripping voltammetry. The electrochemical experiments revealed a certain loss of the electrochemically active surface area of Pt in the catalyst annealed in hydrogen with respect to the original one, while XRD, TEM and XPS indicated only a marginal change in the dispersion of Pt. At the same time, as shown in Fig. 7, hydrogen exposure experiments combined with XPS demonstrated the presence of Mo species directly adsorbed on the Pt surface. Thus the loss of the electrochemically active surface area can be interpreted as the result of partial blocking of Pt surface sites by a Mo-containing encapsulation layer.

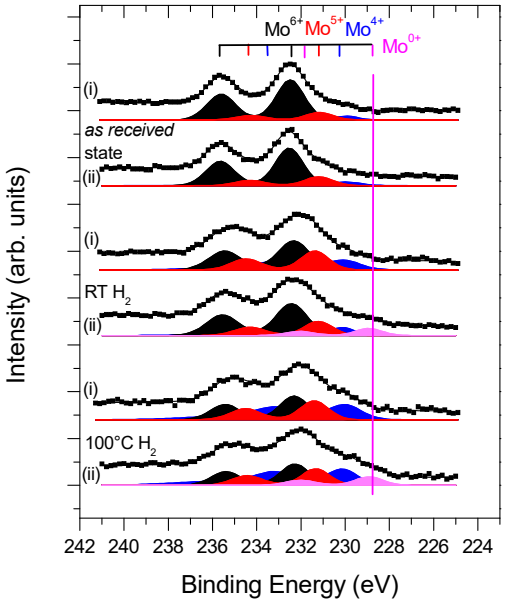

Fig. 7. Mo 3d spectra of the Pt/50C (curves denoted as (i)) and the Pt/50C-250H (curves denoted as (ii)) electrocatalysts measured during *the in situ* hydrogen exposure series (initial state, room temperature and 100°C hydrogen exposure). The assignment of the Mo chemical states is shown on the bar above the graphs.

According to these results, the features of SMSI appear in the Pt/$Ti_{(1-x)}Mo_xO_2$-C electrocatalysts already after a hydrogen treatment at the relatively low 250 °C temperature. An important feature of the hydrogen treated catalyst is its good long term stability, while the unique CO-tolerant property ensured by the composite support remained unchanged. These results confirm that utilization of the strong metal support interaction phenomenon can be a valuable approach for improving the stability of the mixed oxide – carbon composite supported electrocatalysts.

Effect of the reductive treatment on the state and electrocatalytic behavior of Pt in catalysts supported on $Ti_{0.8}Sn_{0.2}O_2$-C composite ($Ti_{0.8}Sn_{0.2}O_2$/C= 75/25) was also investigated. XPS combined with *in situ* H_2 exposure suggested formation of a Sn-Pt alloy after a reductive treatment above 200 °C in both catalysts. Segregation and oxidation of Sn was observed after oxygen exposure of the alloyed catalysts. The electrocatalytic properties and the stability of the initial and reduced catalysts were analyzed by cyclic voltammetry, CO_{ads}-stripping voltammetry and oxygen reduction reaction measurements in order to evaluate the effect of alloying and formation of tin oxide species on the Pt surface in oxidizing environments on their performance. The different oxide microstructure of the two systems allowed assessing its effect on the electrocatalytic behavior, especially during 10,000 cycle long term stability tests.

These observations will form the base for the PhD theses “Assessment of the role of strong metal support interaction (SMSI) on electrocatalytic performance of supported Pt catalysts” of Maria Cristina Silva Cisneros, who is now a PhD student of the George Oláh Doctoral School of Budapest University of Technology and Economics.

2.1.5 Effect of the type of oxophilic metal (M: Mo, Nb, Sn) on the electrocatalytic behavior of the Pt/$Ti_{(1-x)}M_xO_2$-C catalysts

The purpose of detailed electrochemical characterization performed on platinum catalysts supported on a $Ti_{(1-x)}M_xO_2$-C (M: Mo, Nb, Sn) composites was to elucidate the effect of various oxophilic metals (**M**) on CO tolerance, activity and stability. The key element of the concept was the introduction of corrosion resistant mixed oxide-based composite support materials to replace the carbon support in the corrosion-sensitive Pt/C electrocatalysts.

According to the half-cell results, three the most stable TiO_2-rutile-based 20 wt.% Pt/$Ti_{0.8}Mo_{0.2}O_2$-C (C: Vulcan, BP and F-BP) electrocatalysts with $Ti_{0.8}Mo_{0.2}O_2$/C= 25/75 mass ratio can be recommended for use on the anode side of MEA in PEM fuel cell. In order to assess the influence of the support in our recent study [10] the electrocatalytic activity of these catalysts in hydrogen oxidation reaction (HOR) and in ORR were compared with a commercial Pt/C reference

catalyst by rotating disc electrode (RDE) technique. It has been demonstrated that the performance of composite supported catalysts prepared using different carbonaceous materials was nearly identical, while the reference Pt/C catalyst shows a slightly lower activity. Nevertheless, it should be noted, that the BP-based catalysts demonstrated the best stability during 10,000-cycle long-term stability test.

The kinetic parameters related to ORR performance determined using Koutecky-Levich (K-L) plot suggested 4-electron transfer per oxygen molecule leading to the formation of H_2O. The similarity between the Tafel slopes suggested the same reaction mechanism for these electrocatalysts. Smaller limiting current density observed on oxide-containing can be originated from slower diffusion of O_2 through the oxide layer covering the Pt nanoparticles.

The efficiency of the composite-supported electrocatalysts in the HOR was independent of the type of carbonaceous material used, while the reference Pt/C catalyst showed slightly lower limiting current density. The slope of the K-L plots was rather similar and close to the theoretical value: 6.2×10^{-2} and 7.1×10^{-2} (mA/cm^2) rpm$^{-1/2}$ on the V-containing (Pt/C and Pt/75V) and BP-containing (Pt/75BP and Pt/75F-BP) catalysts, respectively.

Comparison of the electrocatalytic characteristics of Mo- and Sn-containing 20 wt.% $Pt/Ti_{0.8}M_{0.2}O_2$-C electrocatalysts with a high carbon content (75 wt.%) was presented in Fig. 8. As shown in Fig. 8.A and 8.B the shape of the CO_{ads} stripping voltammograms and the position of the main CO stripping peak obtained before and after 500-cycle stability test were quite similar. A slight difference was the presence on the CO_{ads}-stripping voltammograms of the Sn-containing supported catalyst of an additional shoulder at 675 mV.

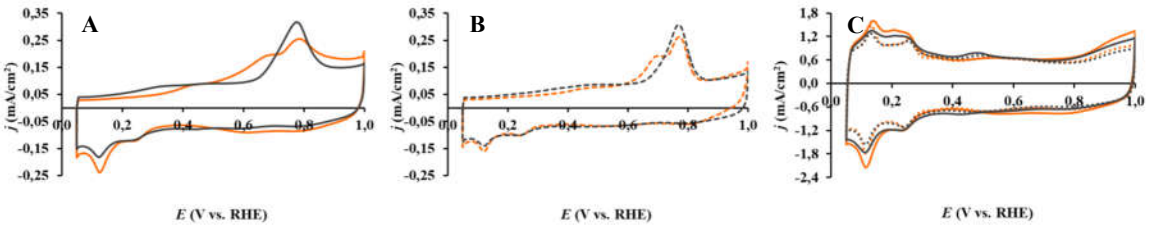

Fig. 8. Comparison of electrocatalytic performance of 20 wt.% $Pt/Ti_{0.8}M_{0.2}O_2$-C (M: Mo (■) and Sn (■)) electrocatalysts with high carbon content (75 wt.%): CO_{ads}-stripping voltammograms obtained before (A) and after the 500-cycle stability test (B); (C) comparison of the cyclic voltammograms obtained on fresh samples (solid lines) and after stability test (dotted lines). Recorded in 0.5 M H_2SO_4 at 10 mV/s (A, B) and 100 mV/s (C), T= 25 °C.

In addition, as can be seen from CVs presented in Fig. 8.C, both catalysts have quite similar electrochemically active Pt surface area. This comparison shows that Sn-containing electrocatalysts can also be promising CO-tolerant anode catalysts for potential use in PEM fuel cells. It should be noted that the specific surface area of Sn-containing samples was even higher compared to the Mo-containing composites with similar composition (S_{BET}= 248 m^2/g and between 373-438 m^2/g for $75Ti_{0.8}Mo_{0.2}O_2$-25BP and $75Ti_{(1-x)}Sn_xO_2$-25BP, respectively).

To clarify the possibility of using Sn-containing catalysts $Pt/Ti_{(1-x)}Sn_xO_2$-C catalysts (x: 0.1-0.3) with a mass ratio of $Ti_{(1-x)}Sn_xO_2$/C= 25/75 and 75/25 as an anode or cathode in PEM fuel cells, their electrocatalytic performance in the HOR and the ORR has also been investigated. The high activity of Sn-containing platinum catalysts in the HOR is evidenced by more sharp increase of current compared to the reference Pt/C catalyst. The ORR polarization curves obtained for the $Pt/Ti_{0.8}Sn_{0.2}O_2$-C electrocatalysts with 75 wt.% carbon content almost coincide with the curves obtained for the commercial Pt/C catalyst (similar onset potential and limiting currents) [8].

Our recent studies have shown that Nb-containing catalysts do not have the ability to oxidize CO at low potentials. However, we have recently demonstrated that $Pt/Ti_{0.93}Nb_{0.07}O_2$-C catalysts with complete Nb incorporation into the TiO_2 lattice have appropriate stability and increased activity in the ORR in acidic medium. Thus, in the future our Nb-containing composite supported catalysts may be recommended for use on the cathode side.

Based on above results requirements for multifunctional composite supports and electrocatalysts to achieve high CO tolerance and stability could be formulated [3].

2.1.6 Scale-up of the preparation of the best electrocatalysts

This research describes design and preparation of the $Ti_{0.8}Mo_{0.2}O_2$–C composite supported Pt catalysts with the mass ratio of the mixed oxide to the carbonaceous materials of 75:25 along with single fuel cell measurements performed using different gas conditions, Pt loadings and operational parameters [11]. Although catalysts with high carbon content are more stable, we have previously demonstrated that composites containing 75 wt.% mixed oxide exhibit better CO-tolerant behavior, which is due to the fact that the number of close contacts between surface Mo particles and Pt nanoparticles is higher. This was the reason why in these studies we used catalyst with $Ti_{0.8}Mo_{0.2}O_2$/C= 75/25 mass ratio.

In the first step, the preparation of promising 20 wt.% Pt/25$Ti_{0.8}Mo_{0.2}O_2$-75BP anode catalysts on an enlarged scale has been carried out. Using multistep sol-gel synthesis, 1 g of composite support materials can be reproducibly obtained in one run.

The Pt-loading method gave the best results (in term of Pt dispersion and uniformity) with 0.2 g of composite support material in one run. An appropriate amount of electrocatalysts sufficient for detailed characterization by various techniques has been obtained in four – five batches. Characterization of different batches of Pt electrocatalysts by cyclic voltammetry was done before unifying them. Our reduction-deposition method applied for Pt deposition provides good reproducibility of the Pt loading for different batches.

According to the results of XRD measurements (Fig. 9.A) in up-scaled composite materials before and after HTT (samples 1 and 2) only the reflections of the TiO_2-rutile crystallites were observed; no reflections characteristic to Mo oxides were found. The changes in the lattice parameters of the rutile phase obtained after HTT (a= 4.640 Å, c= 2.935 Å; pure rutile TiO_2: a= 4.593 Å, c= 2.959 Å) confirm the incorporation of Mo into TiO_2-rutile lattice. Pt loading resulted in the appearance of the reflections of the fcc structure of Pt (Fig. 9.A, sample 3). The uniform distribution of the Pt particles with mean particle size of 3.0 nm ± 0.8 nm was demonstrated by TEM (Figure 9.B).

As shown in Figs. 9.C and 9.D very small performance loss was observed during the electrochemical stability tests for 500 polarization cycles on the composite supported Pt catalyst. After 500 cycles, the loss in electrochemically active Pt surface area ($\Delta ECSA = \{1-(ECSA_{500}/ECSA_1)\}\times 100\%$) calculated from the charges originated from the hydrogen adsorption/desorption in the 1st and 500th cycles was only 8.9 ± 0.5 %. Fig. 9.D shows that the 20 wt.% Pt/$Ti_{0.8}Mo_{0.2}O_2$-C catalyst ensures enhanced CO tolerance compared to the reference commercial 20 wt.% Pt/C (QuinTech) catalyst. The oxidation of CO on the composite supported Pt catalyst commenced at exceptionally low potential values (ca. 50 mV). The maximum of the main CO oxidation peak on the Pt/$Ti_{0.8}Mo_{0.2}O_2$-C catalyst is located at 715 mV, while in the case of the Pt/C catalyst the corresponding peak is around 800 mV.

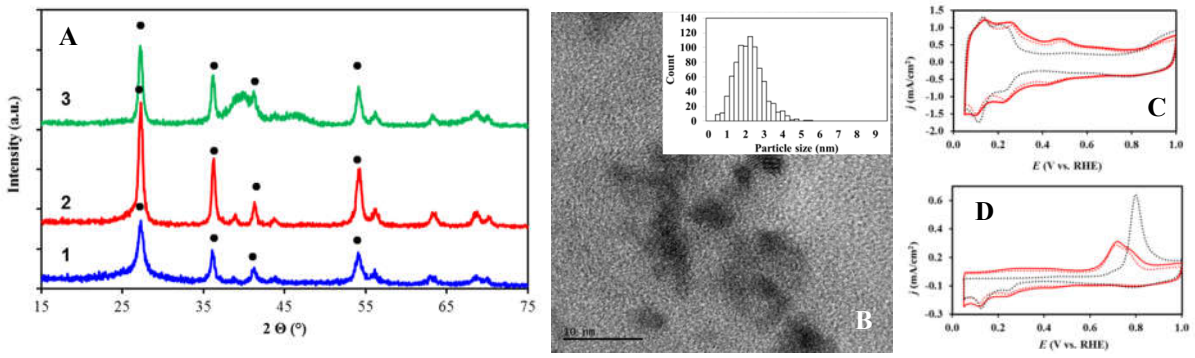

Fig. 9. (A) XRD patterns of $Ti_{0.8}Mo_{0.2}O_2$-C composites before HTT in Ar (sample 1), after HTT (sample 2) and after Pt loading (sample 3). ●- Rutile. (B) TEM images and histogram of particle size distribution for the 20 wt.% Pt/$Ti_{0.8}Mo_{0.2}O_2$-C electrocatalyst. (C) CVs and (D) Ar-purged CO_{ads}-stripping voltammograms of the 20 wt.% Pt/$Ti_{0.8}Mo_{0.2}O_2$-C catalyst recorded before (red solid line) and after 500 cycles of the stability test (red dotted line). Results obtained of the fresh 20 wt.% Pt/C (QuinTech) catalyst (black dotted line) was given for comparison on figures (C) and (D). Obtained in 0.5 M H_2SO_4 at 100 mV/s (C) and 10 mV/s (D), T= 25 °C.

Thus, studies of the structure, composition and the results of CO_{ads} stripping confirmed that the mixed oxide composite support and the electrocatalyst prepared for this study show the well-documented characteristics of the $Pt/Ti_{1-x}Mo_xO_2$-C systems and $Pt/Ti_{0.8}Mo_{0.2}O_2$-C catalyst with $Ti_{0.8}Mo_{0.2}O_2$/C=75/25 mass ratio is suitable for further investigation as an anode in reformate-fed PEM fuel cells. $Pt/Ti_{0.8}Mo_{0.2}O_2$-C anode catalysts with Pt content of 10 and 40 wt.% in the amount of 1 g were also prepared by the same procedure.

2.2 Development of new generation Membrane Electrode Assemblies (MEA)

MEA structures in PEMFCs working with reformate gas differ compared to fuel cells operating with pure hydrogen. MEAs have been developed based on these differences. For fuel cell tests, different approaches (2-layer catalyst, selection of optimal Nafion and Pt loading amounts) have been applied. Within the scope of the project more than 20 catalyst/loading combinations were produced in 5 cm^2 and 15 cm^2 active area membrane electrode sizes and used in the tests.

$Pt/Ti_{0.8}Mo_{0.2}O_2$-C anode catalysts with Pt content of 10, 20 and 40 wt.% were loaded by Turkish partner with 0.25, 0.5, 0.85 and 1.5 mg/cm^2 of Pt onto the gas diffusion layer (GDL) by ***painting method***. In all cases, the 20 wt.% Pt/C with Pt loading of 0.6 mg_{Pt}/cm^2 was used as the cathode. For comparison, MEAs containing state-of-the-art CO tolerant PtRu/C catalyst (Pt: 20 wt.%, Ru: 40 wt.%) with 0.3, 0.58, 0.85, 1.4 and 2.1 mg_{PtRu}/cm^2 loadings were also prepared. Nafion® XL was used as the membrane and Sigracet 29BC was used as the GDL.

In novel two-layer catalyst approach, the first layer deposited onto the GDL contains our CO-tolerant composite supported Pt catalyst and a commercial 20 wt.% Pt/C catalyst, that is in contact with the membrane, was applied in the second layer. Layered (Multiple) catalyst concept has been demonstrated experimentally by Turkish partner.

Moreover, we developed a protocol for the ***spray coating method***, in which catalyst ink was painted by airbrush (AB200) onto the surface of GDLs. The optimal characteristics (1 A/cm^2 at 0.65 V) of a reference MEA developed using minimal amount of commercial 20 and 40 wt.% Pt/C QuinTech catalysts were achieved using 0.15 and 0.05 mg/cm^2 Pt at the cathode (***c***) and anode (***a***), respectively.

Based on the half-cell results three 20 wt.% $Pt/Ti_{0.8}Mo_{0.2}O_2$-C catalysts (C: V, BP and F-BP) with $Ti_{0.8}Mo_{0.2}O_2$/C = 25/75 mass ratio were chosen for the anode side, while commercial 40 wt.% Pt/C was applied as the cathode. According to our preliminary studies, the best performance and the lowest ohmic resistance were observed on the Vulcan-containing composite supported Pt catalyst. However, the BP-based catalyst demonstrated better stability.

2.3 Electrochemical single fuel cell and 5-cell stack assembly & operation

2.3.1 Effect of the reformate gas composition and pressure on the CO tolerant properties of $Pt/Ti_{0.8}Mo_{0.2}O_2$-C electrocatalyst for PEM fuel cells

The MEAs prepared by both partners using various anode catalysts in different variations were tested in Turkey for efficiency and durability under conditions of pure hydrogen, CO-free and 25, 50, 75, and 100 ppm CO-containing reformate gas. Effect of Pt loading, Nafion content, operating temperature, pressure and humidity conditions on the impedance/polarization curves obtained in the presence or absence of CO in reformate and in pure H_2 was demonstrated. Material characteristics were obtained by hundreds of 5 cm^2 single cell tests. By collecting voltage-current, temperature, humidity and impedance data, performance conclusions were drawn.

Polarization measurements were taking with following gas compositions: **H_2** (pure hydrogen), **R** (Reformate without CO, 16% CO_2, 8% CH_4, 42% H_2, balanced N_2), **R-CO** (Reformate with CO, 25 ppm CO, 16% CO_2, 8% CH_4, 42% H_2, balanced N_2) and 100 ppm CO balanced with hydrogen.

Effect of different gas compositions on current at 0.5 V observed during measurements in the fuel cell is shown in Fig. 10 [11].

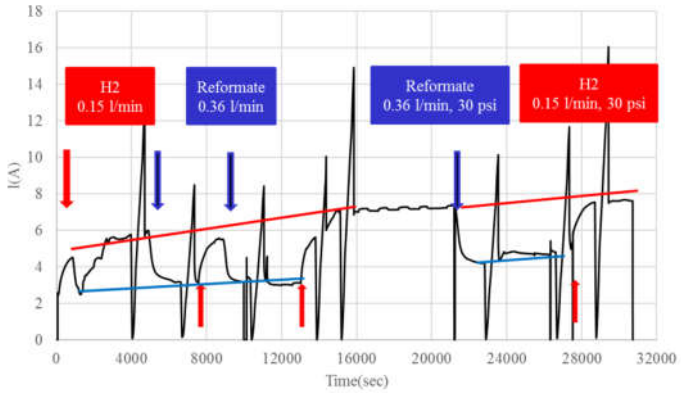

Fig. 10. Change of current with time under 0.5 V polarization for 5 cm^2 single-cell with 0.85 mg_{Pt}/cm^2 loaded 20 wt.%Pt/$Ti_{0.8}Mo_{0.2}O_2$-C anode. Cell temperature: 80 ºC, 100 % RH.

As shown in Fig. 10, when gas was switched from hydrogen to reformate with 25 ppm CO, current was reduced. Switching back to hydrogen allowed current recovery indicating poisoning by CO was temporary. We demonstrated recently [11] that other strategies, i.e. pressure increase, helped as well for further improvement in getting higher current after 10 hours of operation. In addition, higher temperatures and humid conditions were all favorably for increased performance of the catalysts. Polarization results indicated catalyst was performing well with 25 ppm CO, especially at higher cell back-pressures. Dilution of hydrogen with CO_2 and CH_4 had limited negative impact on the performance. It has been demonstrated [11] that catalyst loading of 0.85 mg_{Pt}/cm^2 was effective to give 1000 mA/cm^2 current density at 0.6 V under 25 ppm CO.

The optimal loading of catalysts with 10, 20 and 40 wt.% of Pt was determined based on the correlation between Pt loading, catalyst layer thickness and current density. The effect of loading on the performance of all electrocatalysts developed within the scope of the project is given in Fig. 11. As shown in Fig. 11, in pure hydrogen, irrespective of the Pt content in the catalysts, the best results were obtained on the MEAs with 0.5 mg/cm^2 Pt loading on anode side. An increase in Pt loading, leads to an increase of the thickness of the catalyst layer, while the current density passes through a maximum.

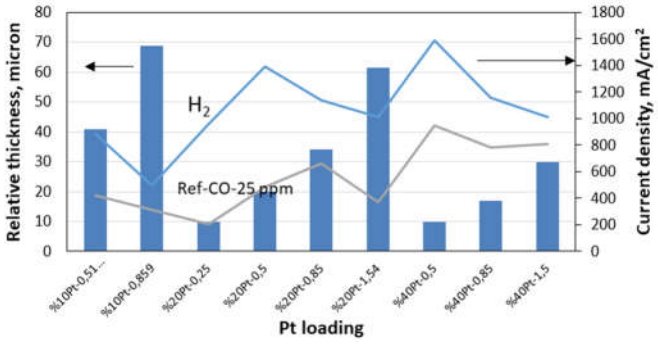

Fig. 11. Effect of anode loadings and gas compositions on current densities obtained on 10, 20 and 40 wt.% Pt/$Ti_{0.8}Mo_{0.2}O_2$-C catalysts. Comparison under 0.5 V polarization.

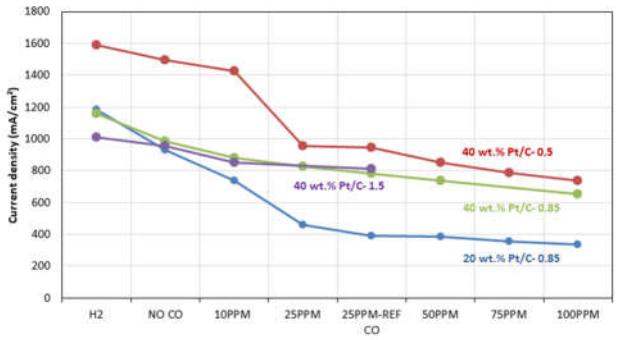

Fig. 12. Effect of different loadings of anode and gas compositions on current densities obtained on 20 and 40 wt.% Pt/$Ti_{0.8}Mo_{0.2}O_2$-C catalysts under 0.5 V polarization.

In the case of testing in a reformate containing 25 ppm CO, this loading of Pt was optimal for catalysts with 10 and 40 wt.% of Pt; the only exception was the catalyst with 20 wt.% Pt, on which the maximum activity was obtained with Pt load of 0.85 mg/cm^2. Loadings above 0.85 mg$_{Pt}$/cm^2 have resulted with lower performance due to thickness increase. According to obtained results it has been concluded that high concentration of Pt in the electrode layer is needed to get higher performance with reasonably low catalyst loading. The small difference between 25 ppm CO in reformat gas and 25 ppm CO in hydrogen, observed in Fig. 12, is most likely due to mass transfer limitation.

The following conclusion was made: (i) the catalyst containing 10 wt.% of Pt was insufficient in elimination of CO poisoning, (ii) the 20 wt.% of Pt catalyst gave the best performance at high loadings (0.85 mg$_{Pt}$/cm^2), (iii) higher Pt loading was more effective with reformate for higher performance and (iv) the best performance was achieved on the 40 wt.% Pt electrocatalyst with 0.5 mg$_{Pt}$/cm^2 at 15 psi pressure and 100% relative humidity for both pure hydrogen and CO-containing fuel.

MEA containing on the anode side 40 wt.% Pt/75Ti$_{0.8}$Mo$_{0.2}$O$_2$-25C catalyst with 0.5 mg$_{Pt}$/cm^2 was compared with MEA build utilizing a commercial PtRu/C catalyst with PtRu content of 0.86 mg/cm^2. A fast and very efficient catalyst accelerated stress test (CAST) involving an application of square-wave from 0.6 to 0.9 V with a 3 sec dwell time at each potential was used in long-term stability tests. Life predictions were made with CAST: CAST results obtained over 200 hours are equivalent to 6000 hours of normal operation. Fuel cell tests with membrane-electrode assemblies containing 0.5 mg$_{Pt}$/cm^2 confirmed the CO tolerance of the composite supported catalysts and indicated stability during an accelerated stress test comparable to that of state-of-the-art commercial CO-tolerant PtRu/C.

In addition, MEAs with very low content of catalysts developed in Hungary (***a:*** 0.05; ***c:*** 0.15 mg$_{Pt}$/cm^2) have been investigated by Turkish partner. The results obtained in pure hydrogen show that in an acidic solution even at loading of 0.05 mg$_{Pt}$/cm^2 hydrogen kinetics is very fast. The influence of the type of carbonaceous material (C: V, BP and F-BP) in the composite on the electrochemical characteristics of related Pt catalysts in PEMFC was evaluated. It has been shown that the dilution of hydrogen with CO_2 and CH_4 in the case of using a CO-free reformate gas has an insignificant negative effect on the operation of catalysts: the smallest current difference in the kinetic and ohmic regions was obtained on the BP-containing catalyst. Nevertheless, anode catalyst loading of 0.05 mg$_{Pt}$/cm^2 was too low to give reasonable performance in the presence of CO impurity in reformate gas.

2.3.2 5-cell stack assembly & operation

After the single cell tests a unique plate design using Solid Works with an active area of 15 cm^2 has been made and a fuel cell stack containing a maximum of 5-cells has been developed by processing on house-made graphite plates. It is produced separately in gaskets suitable for the design; there are cooling channels on the front of the plates and gas flow channels on the back. Fig. 13.A shows electrodes with an active area of 15 cm^2 on the membrane and MEAs sealed with silicone gaskets (Fig. 13.B).

Fig. 13. (A) Electrode with an active area of 15 cm^2 on the membrane, (B) MEAs are sealed with silicone gaskets and (C) stacking.

The stack (Fig. 13.C), created by adding the desired number of cells (from one cell to a stack of 5 cells), was attached to the test station for gas supply and electrochemical measurements. Single cell and stack tests were performed with the developed MEAs. Cells conditioned with hydrogen gas were tested using CO/H_2 gas composition in the range of 10-100 ppm. Due to leaks, 5-cell stack tests could be carried out in a limited time period, mostly 2 and 3-cell stack tests were performed. Using our

catalysts, it has been demonstrated that the sealing improved the performance of the cell operated at 80 °C, and current densities of 1.5 A/cm^2 was achieved with a polarization at 0.6 V. Moreover, after CO poisoning, switching the gas supply from 100 ppm CO/H_2 to hydrogen can completely restore catalyst activity. Accelerated stress tests of the catalysts have also been successfully performed using a 2-cell stack.

Due to the height of the gaskets used between the cells, the pressure was not increased above 5 psi; thus, the breaking of the plates was prevented. Better polarization values were obtained with 10 ppm CO, these values were close to hydrogen polarization. The power values of the 3-cell stack have reached 20 watts.

At the end of the project, 5-cell stack was used to charge a mobile phone (5 V-1 A) by producing 5 watt with 100 ppm CO/H_2 fuel.

3. Utilization possibilities of the results

A possible route for zero emission energy production is utilization of biomass-derived hydrogen in small combined heat and power (CHP) units containing PEMFCs. For wide-range implementation of CHP technologies, it is essential to overcome the high price, the CO poisoning and electrocorrosion sensitivity of the widely used Pt/C. The project addressed the need for highly stable electrocatalysts with long lifetime, low cost and better electrochemical activity along with decreased Pt content. It was demonstrated in a range of experiments (from 3-electrode electrochemical laboratory tests to experiments on 5-cell fuel cell stacks) that transitional metal-doped TiO_2 – active carbon composites are indeed excellent supports for Pt-based catalysts, which provide enhanced stability and tolerance against CO poisoning. Accordingly, these mixed oxide-containing Pt catalysts can be suggested as possible replacement for the PtRu/C combination in CHP applications.

Based on our results, we plan to submit a patent. KONTAKT-Elektro GmbH (Pécs, Hungary), which also produces and distributes fuel cells, showed interest in our new type of catalysts.

The work performed within this project clearly pointed out the added value of the complementary competences of the Hungarian and Turkish partners. We definitely plan further collaboration, involving further proposals, based on this complementarity.

4. Changes in research staff and other relevant information

The research proceeded according to the work plan presented in the proposal. Jamila Rzayeva was employed as a young researcher in the first year of the project. Her task was helping in the characterization of the large number of samples. There was no other personal change.

The equipment used in the segmented fuel cell approach, capable of collecting current and temperature data at 100 different points, which was planned to use by Turkish partner, was broken and no new equipment was budgeted for by the project. With the approval of Turkish Project Office, this task was not implemented.

In the frame of the project, Dr. András Tompos (PI) met with Turkish partners at the 4th International Symposium on Materials for Energy Storage and Conversion (mESC-IS 2019) in Akyaka, Mugla, Turkey between 11-13 September 2019; the Turkish partner did not travel to Hungary. In 2020-2021, due to the outbreak of COVID-19, partners were unable to travel.

5. References

1. I. Borbáth, K. Zelenka, Á. Vass, Z. Pászti, G.P. Szijjártó, Z. Sebestyén, G. Sáfrán, A. Tompos: "CO tolerant Pt electrocatalysts for PEM fuel cells with enhanced stability against electrocorrosion." **International Journal of Hydrogen Energy**, 46 (2021) 13534-13547. Open Access. https://doi.org/10.1016/j.ijhydene.2020.08.002
2. I. Borbáth, E. Tálas, Z. Pászti, K. Zelenka, I. Ayyubov, K. Salmanzade, I.E. Sajó, G. Sáfrán, A. Tompos: "Novel Ti-Mo mixed oxide-carbon composite supported Pt electrocatalysts: Effect of the type of carbonaceous materials." **Applied Catalysis A: General**, 620 (2021) 118155. Open Access. https://doi.org/10.1016/j.apcata.2021.118155
3. I. Borbáth, K. Salmanzade, E. Tálas, Z. Pászti, K. Zelenka, I. Ayyubov, C. Silva, G. Sáfrán, I.E. Sajó, A. Tompos: „Requirements for multifunctional composite supports and electrocatalysts to achieve high CO tolerance and stability". **Book of abstract RomCat 2022**

(13th International Symposium of The Romanian Catalysis Society, June 22-24, 2022, Baile Govora, Romania), pp. 19-20.

4. I. Ayyubov, I. Borbáth, Z. Pászti, Z. Sebestyén, J. Mihály, T. Szabó, E. Illés, A. Domján, M. Florea, D. Radu, A. Kuncser, A. Tompos, E. Tálas: "Peculiarities of graphite oxide derived TiO_2-carbon composites as electrocatalyst supports for polymer electrolyte membrane fuel cells." **Topics in Catalysis**, Accepted: 23 September 2021, published online: 05 October 2021. https://doi.org/10.1007/s11244-021-01513-1
5. I. Ayyubov, A. Vulcu, C. Berghian-Grosan, E. Tálas, I. Borbáth, I. E. Sajó, G. Sáfrán, J. Mihály, András. Tompos: „Preparation of Pt electrocatalyst supported by novel, $Ti_{(1-x)}Mo_xO_2$-C type of composites containing multi-layer graphene." **Reaction Kinetics, Mechanisms and Catalysis**, 135 (2022) 49–69. Open Access. https://doi.org/10.1007/s11144-021-02138-x
6. E. Tálas, I. Ayyubov, A. Vulcu, C. Berghian-Grosan, I. Borbáth, Z. Pászti, Gy. Sáfrán, J. Mihály, Á. Szegedi, A. Tompos: „Use of the ball milling technique in the preparation of potential catalysts for polymer electrolyte membrane fuel cells (PEMFC)". **Book of abstract RomCat 2022** (13th International Symposium of The Romanian Catalysis Society, June 22-24, 2022, Baile Govora, Romania), pp. 21-22.
7. D. Diczházi, I. Borbáth, I. Bakos, G.P. Szijjártó, A. Tompos, Z. Pászti: „Design of Mo-doped mixed oxide–carbon composite supports for Pt-based electrocatalysts: the nature of the Mo-Pt interaction." **Catalysis Today**, 366 (2021) 31–40. https://doi.org/10.1016/j.cattod.2020.04.004
8. I. Borbáth, K. Salmanzade, E. Tálas, Z. Pászti, C. Silva, I.E. Sajó, S. Neatu, A. Kuncser, D. Radu, M. Florea, A. Tompos: „Design of Ti–Sn mixed oxide–carbon composite supports for Pt-based electrocatalysts for polymer electrolyte membrane fuel cells: peculiarities of preparation." **Book of abstract RomCat 2022** (13th International Symposium of The Romanian Catalysis Society, June 22-24, 2022, Baile Govora, Romania), pp. 17-18.
9. C. Silva, I. Borbáth, K. Zelenka, I. E. Sajó, G. Sáfrán, A. Tompos, Z. Pászti: "Effect of the reductive treatment on the state and electrocatalytic behavior of Pt in catalysts supported on $Ti_{0.8}Mo_{0.2}O_2$–C composite." **Reaction Kinetics, Mechanisms and Catalysis,** 135 (2022) 29–47. Open Access. https://doi.org/10.1007/s11144-021-02131-4
10. I. Ayyubov, E. Tálas, K. Salmanzade, A. Kuncser, Z. Pászti, Ș. Neațu, A.G. Mirea, M. Florea, A. Tompos, I. Borbáth: „Electrocatalytic Properties of Mixed-Oxide-Containing Composite-Supported Platinum for Polymer Electrolyte Membrane (PEM) Fuel Cells." **Materials**, 15 (2022) 3671. Open Access. https://doi.org/10.3390/ma15103671
11. M.S. Yazici, S. Dursun, I. Borbáth, A. Tompos: „Reformate gas composition and pressure effect on CO tolerant Pt/$Ti_{0.8}Mo_{0.2}O_2$–C electrocatalyst for PEM fuel cells." **International Journal of Hydrogen Energy**, 46 (2021) 13524-13533. https://doi.org/10.1016/j.ijhydene.2020.08.226